ISBN: 978-3-95450-261-5 ISSN: 2673-7000 doi: 10.18429/JACoW-NAPAC2025-MOP070

PERFORMANCE OPTIMIZATION OF THE IOTA DUOPLASMATRON PROTON SOURCE

N. Banerjee*, D. Edstrom Jr., A. Romanov, M. Wallbank, Fermilab, Batavia, IL, USA
B. Simons, Northern Illinois University, DeKalb, IL, USA

Abstract

We present results from online optimization studies of a duoplasmatron ion source designed to produce 50 keV protons for acceleration to 2.5 MeV and subsequent injection into the Integrable Optics Test Accelerator (IOTA) at Fermilab. Using a Bayesian exploration technique, we developed multi-parameter models of the source's proton current and employed these models to optimize its performance. Depending on the spectrometer configuration used to isolate the proton beam and the chosen optimization objective, we identified three candidate operating points, achieving normalized 50% emittances between 0.57 and 1.3 μm and a maximum proton current of 14.5 ± 0.6 mA.

INTRODUCTION

The Integrable Optics Test Accelerator (IOTA) [1] at Fermilab is transitioning to operations with 2.5 MeV protons in its upcoming run, with the goal of studying beam dynamics in the presence of intense space-charge [2–4] and a controlled impedance environment [5]. To support this, we are commissioning a new injector beamline [6] capable of producing proton beams with currents up to 8 mA, normalized rms transverse emittances of 0.3 – 0.5 μm, and a relative momentum spread of ~ 10^{-3}. Protons are extracted from a duoplasmatron source [7] at 50 keV, accelerated to 2.5 MeV using a 325 MHz normal-conducting Radio Frequency Quadrupole (RFQ) [8], and finally matched into IOTA for single-turn injection. This paper outlines the commissioning and optimization studies of the proton source aimed at achieving the injector's design requirements.

The duoplasmatron source, shown in Fig. 1, is a DC ion source in which hydrogen gas is ionized by a plasma discharge, and the resulting ions are extracted through a pinhole using an electrostatic field. The production of H^+, $H_2{}^+$, and $H_3{}^+$ ions in the plasma cup is driven by impact ionization of neutral hydrogen [9] by hot electrons, which are generated via thermionic emission from a specially coated tungsten filament. The electrons' mean free path and velocity distribution determine the resulting ion species populations. An external magnetic field, aligned with the direction of ion extraction, enhances ion production rates by confining the hot electrons through cyclotron motion. An extractor electrode held at an intermediate potential between ground and the anode is used to extract and focus the ion beam expelled from the pinhole. Because plasma generation in the duoplasmatron produces substantial heat, both the arc discharge and ion extraction are operated in short voltage pulses at a low duty cycle. Table 1 lists the relevant operating parameters of the source along with their acceptable ranges. To optimize proton production, while maintaining control over the beam's transverse phase space and temporal stability, we adjust the hydrogen pressure P_{H_2}, magnetic flux density (via I_{sol}), plasma arc current I_{arc}, and extractor potential.

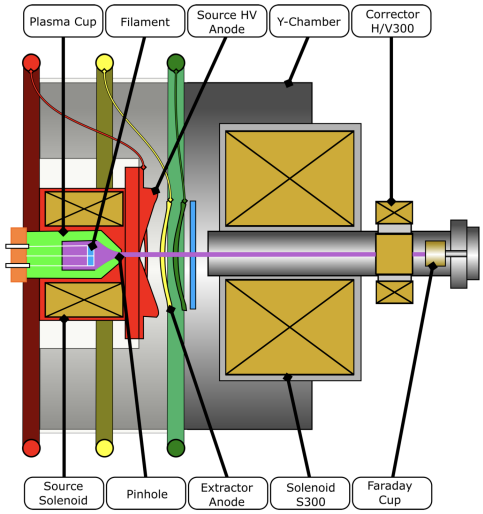

Figure 1: Schematic diagram of the duoplasmatron. The optimization knobs are hydrogen pressure, magnetic field created by the source solenoid, and current driven through the arc discharge inside the plasma cup.

Table 1: Parameter ranges of the IOTA duoplasmatron. The last three parameters are subject to optimization.

Parameter	Nominal	Range	Unit
Anode voltage	50	0 – 50	kV
Filament current	20.5	18 – 22	A
Repetition rate	1	—	Hz
Arc pulse length	80	—	μs
Extractor pulse delay	40	—	μs
Extractor pulse length	40	—	μs
Extractor voltage	10	0 – 10	kV
H_2 pressure (P_{H_2})	—	60 – 250	mTorr
Solenoid current (I_{sol})	—	0.8 – 1.2	A
Arc current (I_{arc})	—	4 – 12	A

In the next section, we describe the spectrometer beamline used to isolate 50 keV protons from the source and present results from a Bayesian exploration of beam current and jitter. We then measure the vertical phase-space

* nilanjan@fnal.gov

ISBN: 978-3-95450-261-5 ISSN: 2673-7000 doi: 10.18429/JACoW-NAPAC2025-MOP070

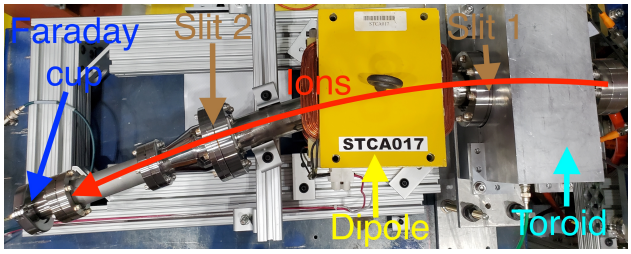

Figure 2: Spectrometer beamline with vertical slits used to characterize the duoplasmatron. The source and the main focusing solenoid are to the right of the image. Later versions remove the toroid and the slits, shorten the beamline, and replace the Faraday cup with an Allison-type emittance scanner.

structure of the proton beam and use Bayesian optimization to increase beam current density at the vertical centroid. Finally, we summarize our results and discuss the potential for applying these techniques to the 2.5 MeV proton beam downstream of the RFQ.

SPECIES OPTIMIZATION

The spectrometer beamline shown in Fig. 2 is used to isolate protons from other ion species and thereby optimize proton production. Ions extracted from the duoplasmatron are focused using a strong solenoid and sent through a toroid for total beam current measurement. Downstream of the toroid, a vertical slit 5 mm wide, centered on the beam pipe axis, selects the core of the horizontal beam distribution. A dipole magnet then disperses the beam horizontally as a function of longitudinal momentum. A second slit, identical to the first and located downstream of the dipole, selects a subset of the dispersed beam, which is then detected by a Faraday cup. This two-slit configuration enables clear separation of ion species, depending on the dipole current. Panel (a) of Fig. 3 shows the resulting ion spectrum, where higher dipole current corresponds to larger ion momentum. At the baseline source configuration, all three peaks corresponding to H^+, $H_2{}^+$, and $H_3{}^+$ in order of increasing dipole current have comparable height. We then adjust the source configuration to maximize the height of the H^+ peak by setting the dipole current to 3.2 A.

To identify the optimal operating configuration, we model proton production in the duoplasmatron as a function of the last three operating parameters listed in Table 1.[1] We apply Bayesian optimization [10] with two objectives: maximizing the temporal mean of the proton current over the last 10 µs of the extractor pulse, and minimizing the current jitter over the same interval. In practice, we use the `BayesianExplorationGenerator` from the `Xopt` [11] package, which prioritizes exploration of the parameter

[1] The extractor voltage primarily controls the initial focusing of the ion beam. We observed that maintaining this voltage at its maximum value yields the highest current.

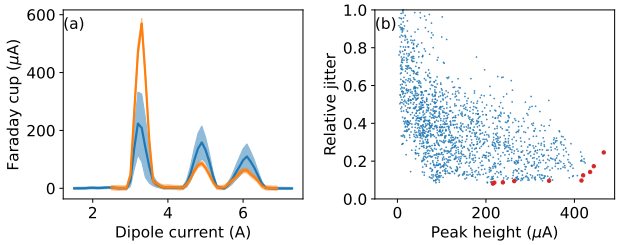

Figure 3: Results of proton current and jitter optimization. (a) Beam current detected on Faraday cup v/s dipole current for two configurations: baseline (blue) and optimized (orange). (b) Relative jitter v/s mean of proton current detected on Faraday cup during Bayesian exploration. Red dots represent the Pareto front.

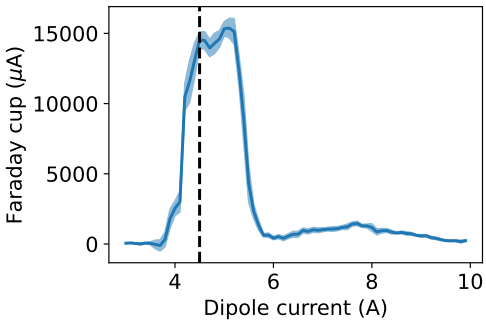

Figure 4: Beam current captured by the Faraday cup as a function of dipole current for the maximum current configuration. The first peak of height 14.5 ± 0.6 mA represents protons selected by the spectrometer.

space over exploitation of current optima. Candidate configurations near the Pareto front, where trade-offs between the two objectives are balanced, are shown as red dots in panel (b) of Fig. 3. The orange curve in panel (a) corresponds to the optimized configuration that increases the H^+ peak while reducing contributions from other species.

Although the ion spectrum obtained with this optimized two-slit setup clearly indicates enhanced proton production, it does not provide a reliable estimate of total proton current. To address this, we modified the spectrometer by removing the toroid and slits and shortening the beamline to increase the phase-space fraction intercepted by the Faraday cup. Starting from the optimized configuration shown in Fig. 3, we manually fine-tuned the parameters to obtain the results in Fig. 4. The resulting ion spectrum no longer resolves three distinct peaks, but the relative spacing of features in the dipole current allows identification of the ion species. Based on this, we conclude that the first peak located at a dipole current of 4.5 A and reaching a height of 14.5 ± 0.6 mA is generated by protons.

ISBN: 978-3-95450-261-5 ISSN: 2673-7000 doi: 10.18429/JACoW-NAPAC2025-MOP070

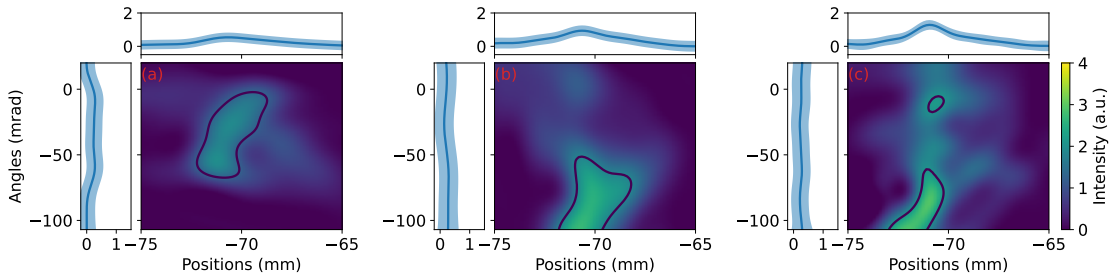

Figure 5: Comparison of vertical phase-space obtained using an Allison-type emittance scanner for 3 configurations. (a) Maximum proton current while minimizing jitter. (b) Maximum proton current only. (c) Maximum intensity at beam centroid. The contour lines contain 50% of the beam. Data for the plots are combined from multiple scans, and smoothened using Gaussian Process models.

PHASE-SPACE OPTIMIZATION

The configuration of the duoplasmatron, along with the optics of the Low Energy Beam Transport (LEBT), provides the most sensitive control parameters for minimizing the transverse emittance of the proton beam injected into IOTA. As a first step in commissioning, we measure and optimize the vertical phase space of the beam emerging from the duoplasmatron. To do this, we replace the Faraday cup in the spectrometer setup (previously used to measure proton current) with an Allison-type emittance scanner [12]. This device allows for time-resolved measurements of the vertical phase-space projection. Figure 5 presents the temporal mean of the beam distribution as a function of vertical position and angle over the last 20 µs of the extractor pulse, for three different duoplasmatron configurations.[2] Each plot shows the expectation value from a Gaussian process model that combines data from multiple runs of the Allison scanner, each with varying resolution across different regions of phase space. The resulting vertical phase-space distributions differ significantly from Gaussian or other common idealized shapes typically used in simulations. Based on this observation, we choose the 50% fractional emittance as our metric for quantifying vertical phase-space area.

The normalized 50% fractional emittance values for the duoplasmatron configurations corresponding to (i) maximum current with minimum jitter (orange curve in Fig. 3a) and (ii) maximum current (Fig. 4), are 1.31 µm and 1.20 µm, respectively. Our goal is to reduce vertical emittance by maximizing beam brightness at the phase-space centroid, while keeping all focusing elements unchanged. In practice, we configure the emittance scanner to sample at a fixed vertical position of –71 mm and integrate the beam distribution across the full angular range of –107 to +107 mrad for each evaluation of the objective function. Panel (c) of Fig. 5 shows the outcome of this optimization, clearly demonstrating an increase in phase-space density near the centroid. The normalized 50% fractional emittance of this brightness-enhanced configuration is 0.571 µm, representing a twofold reduction in vertical emittance.

[2] The main solenoid strength, dipole field and the extractor voltage are held constant throughout all measurements.

CONCLUSION

We have commissioned and optimized a duoplasmatron proton source for injection into IOTA at Fermilab, achieving up to 14.5 ± 0.6 mA of proton current. Vertical phase-space measurements using an Allison-type emittance scanner revealed non-Gaussian beam distributions, motivating the use of the 50% fractional emittance as a performance metric. By optimizing beam brightness at the centroid, we achieved a twofold reduction in vertical emittance, from 1.2–1.3 µm down to 0.571 µm, without altering downstream focusing elements. These results represent a significant step toward meeting the design requirements of IOTA proton injector and demonstrate the effectiveness of data-driven optimization methods for low-energy beamline commissioning.

The phase-space distribution of the final 2.5 MeV proton beam injected into IOTA will be shaped by all downstream beamline elements, with the RFQ playing a key role by selecting a narrow subset of the source beam composed exclusively of protons. We plan to apply the optimization techniques described in this report using diagnostics available in the Medium Energy Beam Transport (MEBT) line, including a toroid, wire scanner, and an identical Allison-type phase-space scanner. In parallel, we are developing a digital twin of the proton injector [13], which will enable us to reduce the experimental parameter space and more efficiently identify optimal configurations for IOTA proton operations.

ACKNOWLEDGEMENT

This manuscript has been authored by Fermi-Forward Discovery Group, LLC under Contract No. 89243024CSC000002 with the U.S. Department of Energy, Office of Science, Office of High Energy Physics.

ISBN: 978-3-95450-261-5 ISSN: 2673-7000 doi: 10.18429/JACoW-NAPAC2025-MOP070

REFERENCES

[1] S. Antipov *et al.*, "IOTA (Integrable Optics Test Accelerator): Facility and Experimental Beam Physics Program", *J. Instrum.*, vol. 12, T03002, 2017. doi:10.1088/1748-0221/12/03/t03002

[2] V. Danilov and S. Nagaitsev, "Nonlinear accelerator lattices with one and two analytic invariants", *Phys. Rev. Spec. Top. - Accel. Beams*, vol. 13, p. 084002, 2010. doi:10.1103/PhysRevSTAB.13.084002

[3] J. Wieland *et al.*, "Improved measurements of nonlinear integrable optics at IOTA", in *Proc. IPAC'23*, Venice, Italy, May 2023, pp. 3230–3232. doi:10.18429/JACoW-IPAC2023-WEPL052

[4] G. Stancari *et al.*, "Beam physics research with the IOTA electron lens", *J. Instrum.*, vol. 16, no.05, P05002, 2021. doi:10.1088/1748-0221/16/05/p05002

[5] R. Ainsworth *et al.*, "A Dedicated Wake-Building Feedback System to Study Single Bunch Instabilities in the Presence of Strong Space Charge", in *Proc. HB'21*, Batavia, IL, USA, Oct. 2021, pp. 135–139. doi:10.18429/JACoW-HB2021-MOP22

[6] D. R. Edstrom *et al.*, "Status of the IOTA Proton Injector", in *Proc. HB'23*, Geneva, Switzerland, Oct. 2023, pp. 629–632. doi:10.18429/JACoW-HB2023-FRA1I1

[7] W. M. Tam, "Characterization of the proton ion source beam for the high intensity neutrino source at Fermilab", Ph.D. thesis, Indiana University, Bloomington, 2010.

[8] P. N. Ostroumov, V. N. Aseev and A. A. Kolomiets, "Application of a new procedure for design of 325 MHz RFQ", *J. Instrum.*, vol. 1, P04002, 2016. doi:10.1088/1748-0221/1/04/P04002

[9] T. Kalvas, "Development and use of computational tools for modelling negative hydrogen ion source extraction systems", Ph.D. thesis, University of Jyväskylä, Jyväskylä, Finland, 2013.

[10] R. Roussel *et al.*, "Bayesian optimization algorithms for accelerator physics", *Phys. Rev. Accel. Beams*, vol. 27, 084801, 2024. doi:10.1103/PhysRevAccelBeams.27.084801

[11] R. Roussel *et al.*, "Xopt: A simplified framework for optimization of accelerator problems using advanced algorithms", in *Proc. IPAC'23*, Venice, Italy, May 2023, pp. 4847–4850. doi:10.18429/JACoW-IPAC2023-THPL164

[12] R. D'Arcy *et al.*, "Characterisation of the PXIE Allison-type emittance scanner", *Nucl. Instrum. Methods Phys. Res. A*, vol. 815, pp. 7–17, 2016. doi:10.1016/j.nima.2016.01.039

[13] N. Kuklev *et al.*, "Deterministic differentiable digital twin for the IOTA/FAST facility", presented at NAPAC'25, Sacramento, CA, USA, Aug. 2025, MOP028, this conference.